Journal of Biotechnology 253 (2017) 23–33

Contents lists available at ScienceDirect

Journal of Biotechnology

journal homepage: www.elsevier.com/locate/jbiotec

Albumin-binding domain from *Streptococcus zooepidemicus* protein Zag as a novel strategy to improve the half-life of therapeutic proteins

Cátia Cantante[a], Sara Lourenço[b], Maurício Morais[c], João Leandro[a], Lurdes Gano[c], Nuno Silva[a], Paula Leandro[a], Mónica Serrano[d], Adriano O. Henriques[d], Ana Andre[e], Catarina Cunha-Santos[a], Carlos Fontes[e], João D.G. Correia[c], Frederico Aires-da-Silva[b,e,*], Joao Goncalves[a,**]

[a] *Research Institute for Medicines (iMed.ULisboa), Faculty of Pharmacy, Universidade de Lisboa, Lisbon, Portugal*
[b] *Technophage, SA, 1649-028 Lisbon, Portugal*
[c] *Centro de Ciências e Tecnologias Nucleares, Instituto Superior Técnico, Universidade de Lisboa, 2695-066 Bobadela LRS, Portugal*
[d] *Instituto de Tecnologia Química e Biológica (ITQB), Universidade Nova de Lisboa, 2780-157 Oeiras, Portugal*
[e] *CIISA—Faculdade de Medicina Veterinária, Universidade de Lisboa,1300-477 Lisbon, Portugal*

ARTICLE INFO

Keywords:
Antibody engineering
Recombinant antibodies
Half-life extension
Albumin binding domain
Streptococcus
ZAG protein

ABSTRACT

Recombinant antibody fragments belong to the promising class of biopharmaceuticals with high potential for future therapeutic applications. However, due to their small size they are rapidly cleared from circulation. Binding to serum proteins can be an effective approach to improve pharmacokinetic properties of short half-life molecules. Herein, we have investigated the Zag albumin-binding domain (ABD) derived from *Streptococcus zooepidemicus* as a novel strategy to improve the pharmacokinetic properties of therapeutic molecules. To validate our approach, the Zag ABD was fused with an anti-TNFα single-domain antibody (sdAb). Our results demonstrated that the sdAb-Zag fusion protein was highly expressed and specifically recognizes human, rat and mouse serum albumins with affinities in the nanomolar range. Moreover, data also demonstrated that the sdAb activity against the therapeutic target (TNFα) was not affected when fused with Zag ABD. Importantly, the Zag ABD increased the sdAb half-life ~39-fold (47 min for sdAb versus 31 h for sdAb-Zag). These findings demonstrate that the Zag ABD fusion is a promising approach to increase the half-life of small recombinant antibodies molecules without affecting their therapeutic efficacy. Moreover, the present study strongly suggests that the Zag ABD fusion strategy can be potentially used as a universal method to improve the pharmokinetics properties of many others therapeutics proteins and peptides in order to improve their dosing schedule and clinical effects.

1. Introduction

Recombinant antibody fragments such as antigen-binding fragments (Fabs), single-chain variable fragments (scFvs) and single-domain antibodies (sdAbs) have been under investigation and development with promising results for clinical applications (Aires da Silva et al., 2008). However, owing to their low molecular weight (< 60 kDa) they usually have short half-life's ranging from a few minutes to a few hours. Consequently, high doses and repeated administration are necessary to maintain their therapeutic activity (Kontermann, 2016, 2011; Strohl, 2015). Within this context, over the past years several efforts have been undertaken towards the development and implementation of half-life extension strategies to prolong the circulation time of these molecules and consequently improve their pharmacokinetic properties and therapeutic potential (Kontermann, 2016). Some of these strategies have focused in the increase of their molecular mass and hydrodynamic radius, and consequently in the decrease in the rate of glomerular filtration by the kidney (*e.g.* PEGylation and glycosylation) (Chen et al., 2011; Goel and Stephens, 2010). For instance, conjugation of polyethylene glycol chains (PEGylation) has been successfully applied to prolong the half-life of several recombinant antibodies for clinical use (Goel and Stephens, 2010). Although this approach is an industry-established method, several studies also indicate that PEGylation can lead to reduced antigen binding and bioactivity of the PEGylated

Abbreviations: ABD, albumin binding domain; AUC, area under the curve; FcRn, neonatal Fc receptor; HSA, human serum albumin; IgG, immunoglobulin G; PEG, polyethylene glycol; MSA, mouse serum albumin; RSA, rat serum albumin; TNFα, necrosis factor; sdAb, single-domain antibody

* Corresponding author at: Technophage, SA, Lisbon, 1649-028, Portugal.
** Corresponding author.
E-mail addresses: fasilva@fmv.ulisboa.pt (F. Aires-da-Silva), joaogoncalves@ff.ul.pt (J. Goncalves).

http://dx.doi.org/10.1016/j.jbiotec.2017.05.017
Received 7 December 2016; Received in revised form 20 May 2017; Accepted 22 May 2017
Available online 24 May 2017
0168-1656/

protein (Chen et al., 2011; Schlereth et al., 2005). As an alternative, other half-life extension methods have been developed by exploring the neonatal Fc receptor (FcRn) mediated recycling, responsible for the long half-life of the human immunoglobulin G (IgG, ~21 days) and human serum albumin protein (HSA, ~19 days) (Kontermann, 2009). Essentially, these strategies are based on the fusion to the IgG Fc region and fusion or binding to serum albumin (Kontermann, 2011, 2009). Albumin is the most abundant protein in the blood plasma with a simple molecular structure and high stability in circulation. Therefore, engineering albumin-derived proteins have been a focus of intense research to increase half-life extension of biopharmaceuticals. For example, Dennis and colleagues developed a strategy based on the fusion of an albumin-binding peptide, using peptide phage display libraries to generate peptides with high affinity to albumin (Dennis et al., 2002). One of the selected albumin-binding peptides was fused with a therapeutic Fab leading to an increase in the half-life of 26-fold in mice. In other examples, several albumin-binding antibodies fragments (*e.g.* scFv and sdAbs) have been developed and showed significant improvement in the plasma half-life and pharmacokinetic properties of different therapeutic proteins (Holt et al., 2008; Stork et al., 2009, 2007). Naturally occurring albumin-binding domains (ABD) found in protein G of certain streptococcal strains have also been explored as a potent half-life extension strategy. For instance, protein G of Streptococcus strain G148 contains three homologous albumin-binding domains. Albumin-binding domain 3 (ABD3) has been extensively studied and is composed of 46 amino acid residues (5–6 kDa) forming a left-handed three-helix bundle. Several *in vivo* studies, have demonstrated that fusion of ABD3 to different antibody fragments could increase the terminal half-life in mice from ~ 2 h to ~27 h (Hopp et al., 2010; Stork et al., 2007).

Jonsson and co-workers have described a plasma protein receptor, a protein-G related cell surface protein from *Streptococcus zooepidemicus*, termed protein Zag, which binds to α_2-macroglobulin, serum albumin and IgG (Jonsson et al., 1995). The IgG-binding domains from Zag are homologous to the IgG-binding domains in protein G and the corresponding domains in proteins MIG and MAG from *Streptococcus dysgalactiae*. Protein Zag shows an albumin-binding profile similar to those of protein G (Nygren et al., 1990) and the albumin-binding DG12 protein from a bovine group G streptococcus (Sjöbring, 1992). This Zag albumin binding domain (Zag ABD) is localized in the N-terminus of the Zag protein and consists in a 52 amino acid sequence that shows binding to human, rat, mouse, horse and dog serum albumin (Sjöbring, 1992).

In the present study, we investigated the Zag ABD as a new approach for extension of the circulation time of therapeutic proteins. To validate our strategy and as a proof-of-concept, the Zag ABD was fused with an anti-TNFα VHH camelid derived sdAb. The fusion protein showed specific binding to human, rat and mouse serum albumins and compared with the parental sdAb, exhibited a strong increase in serum half-life in mice to approximately 39-fold. These results demonstrate, for the first time, the ability of this new streptococcal ABD to improve the pharmacokinetic disposition of therapeutic proteins.

2. Material and methods

2.1. Materials

Human serum albumin (HSA) (catalog no. A3782), rat serum albumin (RSA) (catalog no. A6272), mouse serum albumin (MSA) (catalog no. A3139), human (catalog no. H4522) and mouse serum (catalog no. H5905), and pT7-FLAG2 expression vector were acquired from Sigma-Aldrich (USA). Horseradish peroxidase (HRP) conjugated anti-HA monoclonal antibody (HRP-anti-HA-mAb), HRP-conjugated anti-His monoclonal antibody (HRP anti-His mAb), anti-HA affinity matrix, 2,2′-Azino-di-[3-ethylbenzthiazoline sulfonate (6)] diammonium salt (ABTS), tetrazolium salt WST-1 and cOmplete EDTA-free protease inhibitors cocktail were acquired from Roche (Germany). Recombinant human TNFα and Amicon centrifugal filter units were purchased from Millipore (USA). PD-10 columns and G25 Sephadex were acquired from GE Healthcare (UK) and Sigma-Aldrich, respectively. Radioactivity measurements were done on a dose calibrator (Aloka Curiemeter, IGC-3, Japan) or a gamma-counter (Berthold LB 2111, Germany).

2.2. Cloning of recombinant proteins

DNA encoding anti-TNFα camelid VHH sdAb (VHH clone #3E) (Silence et al., 2004) was synthesized by Nzytech adding a *Sfi*I restriction site at 5′ and 3′ ends, for cloning into the pComb3 x plasmid (Barbas et al., 2001). pComb3X contains a leader peptide sequence ompA (LP) and sequences encoding peptide tags for purification (His_6) and detection (HA). A fragment encoding the LP-VHH-His-HA was amplified by PCR with primers HindIII-LP-*SfiI*-F (5′-CCC AAG CTT ATG AAA AAG ACA GCT ATC GCG ATT GCA GTG GCA CTG GCT GGT TTC GCT ACC GTG GCC CAG GCG GCC-3′) and His-HA-KpnI-R (5′-CGG GGT ACC CCG CTA AGA AGC GTA GTC CGG AAC GTC GTA CGG GTA TGC GCC ATG GTG ATG GTG ATG GTG ATG GTG GCT GCC TCC-3′) and subcloned into the HindIII/KpnI restriction sites of pT7-FLAG2 (Sigma) expression vector. To construct the VHH-Zag ABD fusion protein, we generated by PCR a DNA fragment comprising the entire Zag ABD of *S. zooepidemicus* with primers Zag-1 (5′-GAC ATT ACA GGA GCA GCC TTG TTG GAG GCT AAA GAA GCT GCT ATC AAT GAA CTA AAG CAG TAT GGC ATT AGT GAT TAC TAT GTG ACC TTA ATC-3′) and Zag-2 (5′-GTA TGG CAT TAG TGA TTA CTA TGT GAC CTT AAT CAA CAA AGC CAA AAC TGT TGA AGG TGT CAA TGC GCT TAA GGC AGA GAT TTT ATC AGC TCT ACC G-3′), adding SpeI and NcoI restriction sites at the 5′ and 3′ ends of PCR fragments, respectively. The resulting PCR fragments were gel-purified, digested with SpeI/NcoI restriction enzymes and cloned into pT7-VHH vector. A short GS linker (SGGGGS) was used to link the VHH and Zag ABD. The Zag ABD was cloned into the pT7 vector without the VHH and used as control. The VHH, VHH-Zag and Zag constructs (~ 450 bp, ~700 bp and ~250 bp, respectively) were confirmed by standard sequencing methods (Macrogen, South Korea) using the universal T7 primer.

2.3. Expression and purification of proteins

VHH, VHH-Zag and Zag were expressed in *Escherichia coli (E. coli)* strain BL21(DE3). One liter of LB medium supplemented with 100 μg/ml ampicillin was inoculated with 10 ml of overnight bacterial culture transformed with pT7-VHH, pT7-VHH-Zag or pT7-Zag plasmids and growth to exponential phase (A_{600} = ~0.9) at 37 °C. Protein expression was induced with 1 mM of isopropyl β-D-1-thiogalactopyranoside (IPTG) and growth was performed during 16 h at 18 °C. Cells were harvested by centrifugation (4000*g* for 15 min at 4 °C) and resuspended in 50 ml equilibration buffer (50 mM HEPES, 1 M NaCl, 5 mM $CaCl_2$, 30 mM imidazole, pH 7.5) supplemented with protease inhibitors. After cell lysis by sonication, the protein extract was recovered by centrifugation (14,000*g* for 30 min at 4 °C) and filtrated through a 0.2 μm syringe filter. Proteins purification was performed by nickel chelate affinity chromatography using the HisTrap HP columns coupled to an AKTA FPLC System (GE Healthcare). After a washing step (50 mM HEPES, 1 M NaCl, 5 mM $CaCl_2$, 60 mM imidazole, pH 7.5), elution of the recombinant antibody fragments occurred by a linear imidazole gradient from 60 to 300 mM in 50 mM HEPES, 1 M NaCl, 5 mM $CaCl_2$, pH 7.5. Protein fractions were pooled, desalted and concentrated in 50 mM HEPES, 100 mM NaCl, 5 mM $CaCl_2$, pH 7.5 using Amicon 10 K columns (Millipore). Finally, VHH, VHH-Zag or Zag samples were loaded onto a HiPrep 16/60 Sephacryl S-100 HR gel filtration column (GE Healthcare) and pooled fractions were analyzed for protein purity by SDS-PAGE. The protein concentration obtained spectrophotometrically in Nanodrop ND-1000 at 280 nm was used to calculate the ε value of

each protein (εVHH = 34380 l mol − 1 cm − 1; εVHH-Zag = 38850 l mol − 1 cm − 1; εZag = 8940 l mol − 1 cm − 1).

2.4. Size exclusion chromatography

FPLC-SEC determined the apparent molecular weight of the recombinant antibody and formation of antibody/albumin complexes by a HiLoad Superdex 200 HR column (GE Healthcare) with a flow rate of 0.7 ml/min and PBS as running buffer at 4 °C. The following standard proteins were used: apoferritin (443 kDa, R_S 6.1 nm), β-amylase (200 kDa, R_S 5.4 nm), alcohol dehydrogenase (150 kDa, R_S 4.55 nm), bovine serum albumin (67 kDa, R_S 3.55 nm), ovalbumin (45 kDa, R_S 3.05), myoglobin (17.6 kDa, R_S 1.91 nm), ribonuclease A (13.7 kDa, RS 1.64 nm) and cytochrome c (12.4 kDa, R_S 1.77 nm). Proteins blue dextran and l-tyrosine resolved the void and total column volume, respectively. Elution volume of the protein standard determined a standard curve of Stokes' radius (R_S) *versus* $(-\log K_{av})^{1/2}$ that was used to calculate the Stokes radius of recombinant antibody and antibody/albumin complexes. We analyzed the complex formation of VHH-Zag with HSA and MSA by incubating equimolar amounts of VHH-Zag and albumin (10 μM) in PBS at room temperature and subsequent analysis by SEC.

2.5. Binding activity by ELISA

Binding properties of VHH and VHH-Zag proteins were determined in 96-well ELISA plates (Costar, #3690) coated with HSA, RSA, MSA (10 μg/well) and human TNFα (200 ng/well) overnight at 4 °C. After 1 h blocking with 5% soya milk, purified recombinant antibodies were incubated in triplicate for 1 h at room temperature. The binding activity to human TNFα was measured in the presence or absence of HSA (1 mg/ml). HRP-conjugated anti-HA-tag monoclonal antibody was used for detection by measurement of absorbance at 405 nm with ABTS substrate. GraphPad Prism Software version 5 was used for data analysis.

2.6. Affinity measurements

The binding affinities between VHH-Zag and HSA, RSA and MSA were obtained using surface plasmon resonance (SPR) at 25 °C (BIAcore 2000, BIAcore Inc.) Human, rat and mouse albumins were captured on a CM5 chip using amine coupling at ~1000 resonance units. VHH-Zag fusion protein at 0, 10, 50, 100, 200, 300, and 400 nM were injected for 4 min. The bound protein was allowed to dissociate for 10 min before matrix regeneration using 10 mM glycine, pH 1.5. The signal from an injection passing over an uncoupled cell was subtracted from that of an immobilized cell to generate sensorgrams of the amount of protein bound as a function of time. The running buffer, HBS was used for all sample dilutions. BIAcore kinetic evaluation software (version 3.1) was used to determinate K_D from association and dissociation rates using a one-to-one binding model. VHH sdAb and Zag ABD were used as controls.

2.7. Neutralization of TNF-dependent cytotoxic activity

The murine aneuploidy fibrosarcoma cell line (L929) was used as a cytotoxic-mediated assay to measure the anti-TNFα VHH and VHH-Zag blocking effect on TNFα/TNFR (TNF receptor) interaction. Briefly, L929 cells were grown to 90% confluence in Dulbecco's modified Eagle's medium supplemented with 10% fetal bovine serum, penicillin (100 units/ml), streptomycin sulfate (10 μg/ml), and L-glutamine (2 mM). Cells were plated in 96-well plates at a density of 25,000 cell/well and then incubated overnight. Serial dilutions of VHH and VHH-Zag were mixed in triplicates with a cytotoxic concentration of TNFα (final assay concentration 1 ng/ml) or in the absence of this cytokine to measure the cell viability. Actinomycin D was added to a final concentration of 1 μg/ml to increase the cell sensitivity. After at least 2 h of incubation at 37 °C with shaking, the mixture was added to the plated cells. Cells were incubated for 24 h at 37 °C in an atmosphere of 5% CO_2. Cell viability was determined using the tetrazolium salt WST-1 (10 μg/well) from Roche, after at least 30 min of incubation by measuring the absorbance at 450 nm. GraphPad Prism Software version 5 was used for data analysis.

2.8. Protein thermal stability and in vitro serum stability

VHH and VHH-Zag melting temperatures (T_m) were determined using the Protein Thermal Shift Kit and 7500 Fast Real-Time PCR System (Applied Biosystems) according to manufacturer's instructions. The MicroAmp™ Fast Optical 96-well Reaction Plates of all protein samples (5 μg/well) were analyzed in quadruplicate and diluted in 50 mM HEPES, 100 mM NaCl, 5 mM $CaCl_2$, pH 7.5, and Protein Thermal Shift™ Dye 1x. Collected data analyzed with Protein Thermal Shift Software version 1.1 provided the values of protein thermal stability. To evaluate the stability of recombinant antibodies in mouse and human serum, we incubated VHH and VHH-Zag at a concentration of 10 μg/ml for up to 4 days and 24 days, respectively, at 37 °C. ELISA and Western Blot using HRP-conjugated anti-His-tag monoclonal antibody generated the data of *in vitro* stability as described above.

2.9. Pharmacokinetics

Animal care and all pharmacokinetic (PK) studies were conducted according to guidelines for animal care and ethics for animal experiments outlined in the National and European Law. CD-1 mice (Charles River, female, 6–8 weeks, 25–30 g weight; n = 3) were administered with intravenous injections in the tail vein with 25 μg of VHH or VHH-Zag. Serum samples obtained from injected animals at regular intervals of 5, 30, 60, 120, and 360 min, 24, 48 and 72 h, were quantified by ELISA. Briefly, human TNFα was immobilized in 384 well-plates (100 ng/well) overnight at 4 °C. After 1 h blocking with PIERCE blocking, serum samples were titrated in duplicates and incubated for 1 h at room temperature. Detection of VHH and VHH-Zag were performed with HRP-conjugated anti-HA-tag monoclonal antibody by measurement the absorbance at 405 nm with ABTS substrate. As described by Stork and co-workers, determined serum concentrations of TNFα-binding proteins were interpolated to the corresponding calibration curves. For comparison, the first time point (5 min) was set to 100%. The pharmacokinetic parameters area under the curve (AUC), $t_{1/2}\alpha$ and $t_{1/2}\beta$ were calculated with Excel, using the first three time points to calculate $t_{1/2}\alpha$ and the last three time points to calculate $t_{1/2}\beta$.

2.10. Radiolabelling of $^{99m}Tc(CO)_3$-VHH and $^{99m}Tc(CO)_3$-VHH-Zag proteins

$Na[^{99m}TcO_4]$ was eluted from a $^{99}Mo/^{99m}Tc$ generator. The radioactive precursor *fac*-$[^{99m}Tc(CO)_3(H_2O)_3]^+$ was prepared using a IsoLink® kit (Covidien) and its radiochemical purity checked by RP-HPLC and ITLC-SG. The radiolabeled proteins *fac*-$[^{99m}Tc(CO)_3]$-VHH and *fac*-$[^{99m}Tc(CO)_3]$-VHH-Zag were obtained by reacting the recombinant antibodies with *fac*-$[^{99m}Tc(CO)_3(H_2O)_3]^+$. Briefly, a specific volume of the *fac*-$[^{99m}Tc(CO)_3(H_2O)_3]^+$ solution added to a nitrogen-purged closed glass vial containing a solution of the His-tag containing proteins VHH or VHH-Zag resulted in a final concentration of 1 mg/ml. The mixture reacted for 3 h at 37 °C and the radiochemical purity of *fac*-$[^{99m}Tc(CO)_3]$-VHH and *fac*-$[^{99m}Tc(CO)_3]$-VHH-Zag was checked by ITLC-SG (Varian) analysis every hour using a 5% HCl (6 M) solution in MeOH as eluent. $[^{99m}Tc(CO)_3(H_2O)_3]^+$ and $[TcO_4]^-$ migrate in the front of the solvent (Rf = 1), whereas the radioactive antibodies remain at the origin (Rf = 0). A radioactive scanner (Berthold LB 2723, Germany) equipped with 20 mm diameter NaI(Tl) scintillation crystal

detected the radioactivity distribution on the ITLC-SG strips. Radioactivity measurements were done on a dose calibrator (Aloka Curiemeter, IGC-3, Japan) or a gamma-counter (Berthold LB 2111, Germany). Purification of the ^{99m}Tc-radiolabeled antibodies was performed by gel filtration through Shepadex G-25 or PD-10 column, using 20 nM sodium chloride solution as eluent. After radioactive decay (10 half-lives), ELISA assay tested the VHH and VHH-Zag proteins to ensure that their binding capacities were unaffected (data not shown).

2.11. Partition coefficient

The "shake-flask" method evaluated the partition coefficient. In this method, the radioactive antibodies were added to a mixture of octanol (1 ml) and 0.1 M PBS1 x pH 7.4 (1 m), previously saturated with each other by stirring. This mixture was vortexed and centrifuged (3000 rpm, 10 min) to allow phase separation. Aliquots of both octanol and PBS1 x were counted in a γ-counter. The calculated partition coefficient ($P_{o/w}$) resulted from dividing the counts in the octanol phase by those in the buffer, and the results expressed as log $P_{o/w}$ ± SD.

2.12. Biodistribution studies of ^{99m}Tc(CO)$_3$-VHH and ^{99m}Tc(CO)$_3$-VHH-Zag

The *in vivo* evaluation studies of radiolabelled VHH and VHH-Zag were performed in triplicated (n = 3) in healthy female CD-1 mice (Charles River, 6–8 weeks, 25–30 g weight). All animal experiments were performed by the guidelines for animal care and ethics for animal testing outlined in the National and European Law. Animals injected intravenously into the tail vein with 100 µl of the radiolabeled compounds (2.6–3.7 GBq) were sacrificed by cervical dislocation at 5 min, 30 min, 1 h, 4 h and 24 h after injection. The dose administered and the radioactivity in the sacrificed animals was measured using a dose calibrator. The difference between the radioactivity in the injected and that in the killed animals were assumed to be due to excretion. Tissues of interest were dissected, rinsed to remove excess blood, weighed, and their radioactivity was measured. The total activity uptake for blood, bone, muscle, was estimated assuming that these organs constitute 6, 10, and 40% of the total body weight, respectively. Blood and urine were also collected at the sacrifice time and analyzed by ITLC.

3. Results

3.1. Expression and purification of VHH and VHH-Zag

The VHH-Zag construct was generated by fusing the Zag ABD from the Zag *Streptococcus zooepidemicus* surface protein to the anti-TNFα camelid VHH#3E clone (Silence et al., 2004) including histidine (His_6) and HA tags in C-terminal (Fig. 1A and B). The fusion protein obtained presents 235 amino acid residues with a calculated molecular weight of ~25.2 kDa. The VHH was also constructed as described in the material and methods section and used as a control. VHH and VHH-Zag were expressed in *E. coli* BL21 (DE3) and purified by IMAC and gel filtration. SDS-PAGE and Western Blot results showed a single protein band with the expected molecular weights for VHH and VHH-Zag under reducing and non-reducing conditions (Fig. 1C and 1D). After expression and purification of one liter of culture, we obtain 18 ± 2 mg of VHH and 23 ± 2 mg of VHH-Zag. The same profile of protein yields was obtained when Zag ABD was fused in the N-terminal of the VHH (data not shown).

3.2. Binding activity of VHH-Zag against TNFα

After purification, the VHH-Zag binding activity to human TNFα was tested in an ELISA assay. The VHH was used as a control and as shown in Fig. 2, both proteins specifically bound to TNFα. Importantly, VHH-Zag binding to TNFα was similar to the binding of the parental VHH without the Zag domain (Fig. 2A; VHH-Zag binding EC_{50} = 0.130 nM vs VHH binding EC_{50} = 0.100 nM). Moreover, binding of VHH-Zag to TNFα was not affected by the HSA presence (Fig. 2B; VHH-Zag with HSA EC50 = 0.132 nM vs VHH with HSA EC_{50} = 0.118 nM). Thus, the antigen-binding sites in VHH-Zag are accessible for TNFα binding, and the presence of albumin does not interfere with antigen targeting.

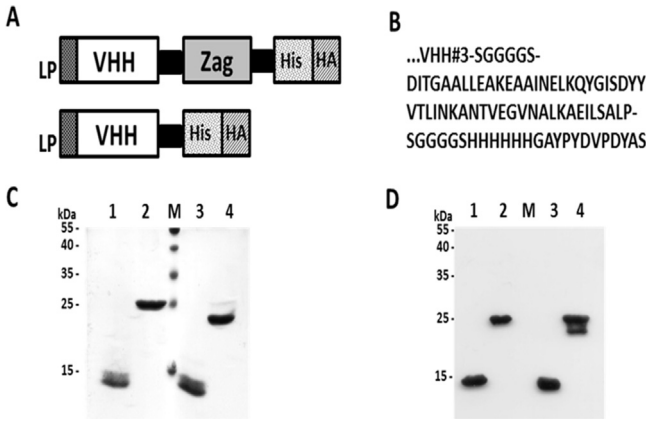

Fig. 1. Construction and expression of VHH and VHH-Zag. (A) Schematic representation of the VHH and VHH-Zag constructs including the N-terminal leader peptide (LP), the C-terminal histidine (His_6) and HA tags. (B) Sequence of the Zag ABD derived from the from *Streptococcus zooepidemicus*. (C) SDS-PAGE and (D) Western Blot analysis of the VHH and VHH-Zag purified proteins (3 µg/lane) under reducing (lanes 1 and 2, respectively) and non-reducing conditions (lanes 3 and 4, respectively). Gels were stained with Coomassie brilliant blue (C) or immunoblotted with HRP conjugate anti-HA mAb (D). (For interpretation of the references to colour in this figure legend, the reader is referred to the web version of this article.

3.3. Binding activity of VHH-Zag to albumins

To determine the relative binding activity of Zag ABD against human, rat and mouse albumins an ELISA was performed (Material and Methods section). As shown in Fig. 3, the VHH-Zag fusion protein specifically bound to human, rat and mouse albumins with a similar profile (HSA EC_{50} = 1.074 ± 0.03 nM; RSA EC_{50} = 1.698 ± 0.06 nM and MSA EC_{50} = 4.354 ± 0.08 nM). After albumin binding confirmation by ELISA, Biacore analyses were performed to evaluate affinities behavior and parameters of the Zag fusion protein. As presented in Fig. 4A–D and Table 1, affinities of VHH-Zag for human, rat and mouse albumins were in the lower nanomolar range. The data showed a higher affinity for HSA and RSA, with K_D of 4.57 nM and 0.42 nM, respectively, when compared with a K_D of 40.6 nM for MSA (Table 1). In contrast, no binding activity against albumins was observed for VHH (Fig. S1, supplementary data). The binding activity was also measured by Biacore for the Zag ABD without the VHH fusion and a similar profile was observed as obtained for the VHH-Zag (Fig. S2 and S3 and Table S1, supplementary data).

To analyze the interaction between VHH-Zag and HSA or MSA in solution, we performed a size exclusion chromatography (SEC) analysis (Fig. 5 and Table S2 supplementary data). VHH-Zag eluted with a dominant peak (65%) corresponding to an apparent molecular mass of 26.4 kDa (R_S 2.59 nm) (Fig. 5A). HSA revealed a major peak (93%) corresponding to the monomeric form with an apparent molecular mass of 68.1 kDa (R_S 3.67 nm) and minor peak (7%) of 163 kDa (Fig. 5B). Incubation of equimolar concentrations of VHH-Zag and HSA shifted the HSA peaks to higher apparent molecular masses, 230.5 kDa (28%) and 101.2 kDa (50%), the later corresponding to a stoichiometry of 1:1 of the complex VHH – Zag/monomeric HSA (R_S 4.16 nm) (Fig. 5C). The unbound VHH-Zag corresponded to ~17%. We obtained similar results

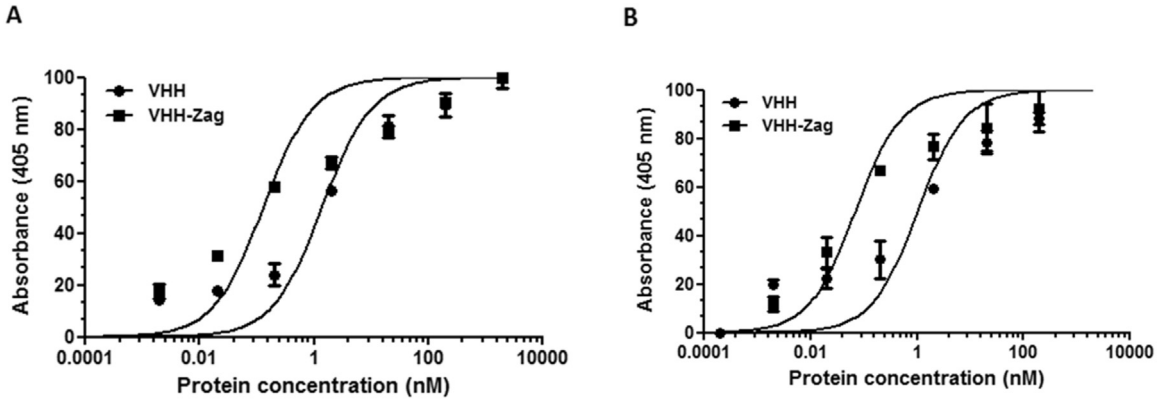

Fig. 2. Binding of VHH and VHH-Zag to human TNFα. ELISA plates were coated with human TNFα and binding of VHH and VHH-Zag fusion protein was measured in the absence (A) and presence (B) of HSA (1 mg/ml). Detection was performed by HRP-conjugated anti-HA mAb. Error bars correspond to standard deviation (n = 3).

for the MSA. However, MSA showed higher molecular mass forms than the human counterpart (Fig. 5D) and a major peak (40%; monomeric form) with an apparent molecular mass of 64.3 kDa (R_S 3.60 nm). Incubation of MSA with VHH-Zag resulted in the shift of the monomeric MSA to 98.6 kDa (R_S 4.01 nm; 26%) (Fig. 5E). Unbound VHH-Zag was slightly higher when compared with human albumin (36%).

3.4. Thermal stability and in vitro serum stability

Thermal stability of VHH and VHH-Zag was calculated using the Protein Thermal Shift Kit and Protein Thermal Shift Software. As depicted in Table 2, the melting temperature (Tm) of VHH-Zag is similar with the Tm presented by the parental VHH, indicating that VHH-Zag is equally thermal stable as VHH. *In vitro* stability was also analyzed by incubation of VHH and VHH-Zag proteins with human or mouse serum at 37 °C for 4 and 24 days and then their integrity analyzed by western-blot. As shown in Fig. 6, both proteins were detected with the expected molecular weights and no degradation was observed. Moreover, the binding activities were confirmed by ELISA in all the samples and were similar to samples before incubation (Day 0) (data not shown).

3.5. Neutralization of TNFα-dependent cytotoxic activity by VHH-Zag

To measure the VHH-Zag blocking effect on TNF-α/TNFR interaction, the murine aneuploid fibrosarcoma cell line (L929) was used in a cytotoxic TNFα-mediated assay as described in the material and methods section. As shown in Fig. 7, both the parental VHH and VHH-Zag fusion protein inhibited the TNFα-induced cell death of L929 in a dose-dependent manner. Importantly, the inhibitory profiles of VHH and VHH-Zag were almost identical, thus indicating that the fusion with the Zag ABD does not interfere with the activity of the anti-TNFα VHH.

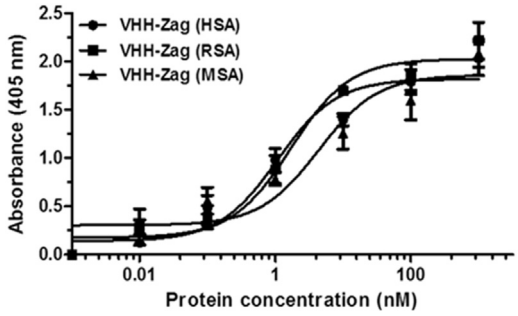

Fig. 3. Binding of VHH-Zag to human, rat and mouse albumin. Binding of VHH-Zag fusion protein was evaluated in ELISA against human, rat and mouse albumins. Bound proteins were detected using an HRP-conjugated anti-HA mAb. Error bars correspond to standard deviation (n = 3).

3.6. Pharmacokinetics and organ biodistribution of VHH and VHH-Zag

To compare the pharmacokinetic properties of VHH and VHH-Zag, CD-1 mices were single injected into the tail vein with 25 μg of protein. Serum concentrations of VHH and VHH-Zag were determined by ELISA at different time points as described in the material and methods section. Compared with VHH, VHH-Zag showed clearly a highly prolonged residence time in blood and remaining organism (Fig. 8 and Table 3), with the terminal half-life ($t_{1/2}\beta$) increasing from 0.79 h (VHH) to 30.55 h (VHH-Zag), corresponding to a 39-fold increase. Moreover, distribution phase half-life ($t_{1/2}\alpha$) showed a 7-fold increase, from 0.52 h (VHH) to 3.21 h (VHH-Zag). Comparison of the AUC also demonstrated the improvement of VHH-Zag pharmacokinetic properties. The $AUC_{(0\text{-}24)}$ for VHH-Zag, increased by a factor of 20 comparing with VHH. A western blot was performed to confirm the presence and identity of VHH and VHH-Zag at each time point. As illustrated in Fig. 9, comparing with VHH (residence in serum during 2 h), VHH-Zag can be detected by immunoblot in mouse serum until 72 h after injection.

In order to compare the biodistribution profile of VHH and VHH-Zag, both proteins were radiolabeled with the "$^{99m}Tc(CO)_3$" core and injected into CD-1 mice. Tissue distribution and *in vivo* stability were monitored over a period of 48 h (Fig. 10 and Tables S3 and S4, supplementary data). For all tested time points, a total of 84–99% of injected activity was recovered. Organ to blood ratio at 24 h (Table S5, supplementary data) showed a very high radioactivity accumulation within the kidney for VHH, with 390 times more concentrated than in the blood. Moreover, biodistribution assay also showed a trend for $^{99m}Tc(CO)_3$-VHH accumulation within the highly perfused organs intestine, muscle, and liver, respectively with 3 times, 5 times and 11 times more concentrated in these organs than in the blood. For the lung and bone $^{99m}Tc(CO)_3$-VHH also showed a 2-fold increase in concentration when compared to blood. For other organs (spleen, heart, stomach and pancreas), VHH showed a lower level when compared to blood. Importantly and in contrast, $^{99m}Tc(CO)_3$-VHH-Zag showed only a slight accumulation within the liver and kidney, with approximately 1.5 times more concentrated in these two organs when compared to blood. For the rest of collected organs, no accumulation was observed. When biodistribution results are normalized to organ weight (Fig. 10, Tables 2 and 3, supplementary data), it is evident the higher radioactivity retention of $^{99m}Tc(CO)_3$-VHH in the kidney when compared to $^{99m}Tc(CO)_3$-VHH-Zag. This finding is in agreement with the predominant urinary excretory route of VHH.

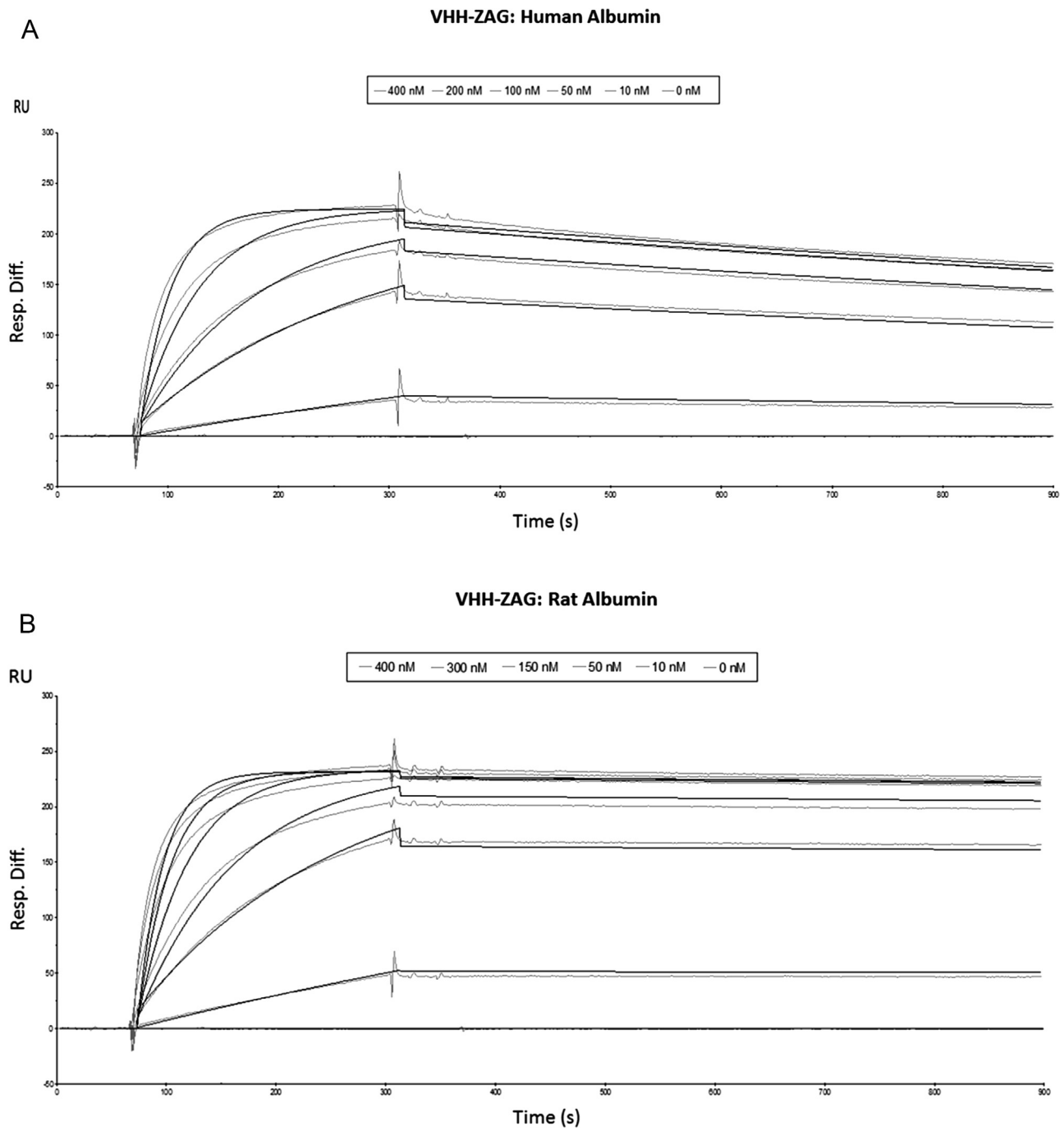

Fig. 4. Affinity measurements by surface plasmon resonance. Shown are Biacore 2000 representative sensorgrams obtained for the VHH-Zag binding against immobilized HSA (A), RSA (B) and MSA (C). The VHH-Zag was injected at different concentrations ranging from 0, 10, 50, 100, 200, 300, and 400 nM. Each concentration was tested in duplicates and VHH used as control. (D) Superimposed sensorgrams observed for VHH-ZAG fusion protein injected at 200 nM against the three albumins (human, rat and mouse).

4. Discussion

Herein, we assessed the ability of the albumin-binding domain (ABD) from streptococcal protein Zag, a protein-G related surface protein, to extend the circulation half-life of therapeutic proteins. For this purpose and to validate our strategy, the Zag ABD was fused with an anti-TNFα VHH single-domain antibody. Our results demonstrate that the Zag ABD could be efficiently fused to the VHH and expressed in *E. coli* in the soluble format and with a high protein yield recovery per liter. Moreover, when we compared the protein yields with the parental VHH, we observed that higher yields were obtained when the ABD was fused with VHH. This behavior was also observed when the Zag ABD was fused with other sdAbs that we are developing in our laboratory (data not shown). So, it seems that the Zag ABD is extremely soluble and can increase the protein yields when fused to the therapeutic protein. These properties can be a benefit in terms of production and process development in future scale up process. In terms of binding activity we confirmed by ELISA that the VHH-Zag fusion protein specifically recognizes the human TNFα and human, rat and mouse serum albumins. Importantly, we demonstrate that the presence of HSA did not affect the binding of VHH-Zag to human TNFα, showing similar values to the VHH alone. These results indicate that VHH-Zag is active when exposed to the therapeutic target (TNFα) in the presence of albumin. Moreover, when we measured the Zag ABD binding profile by surface plasmon resonance to human, rat and mouse albumins, we obtained affinities in the nanomolar range, with values of 4.57, 0.42

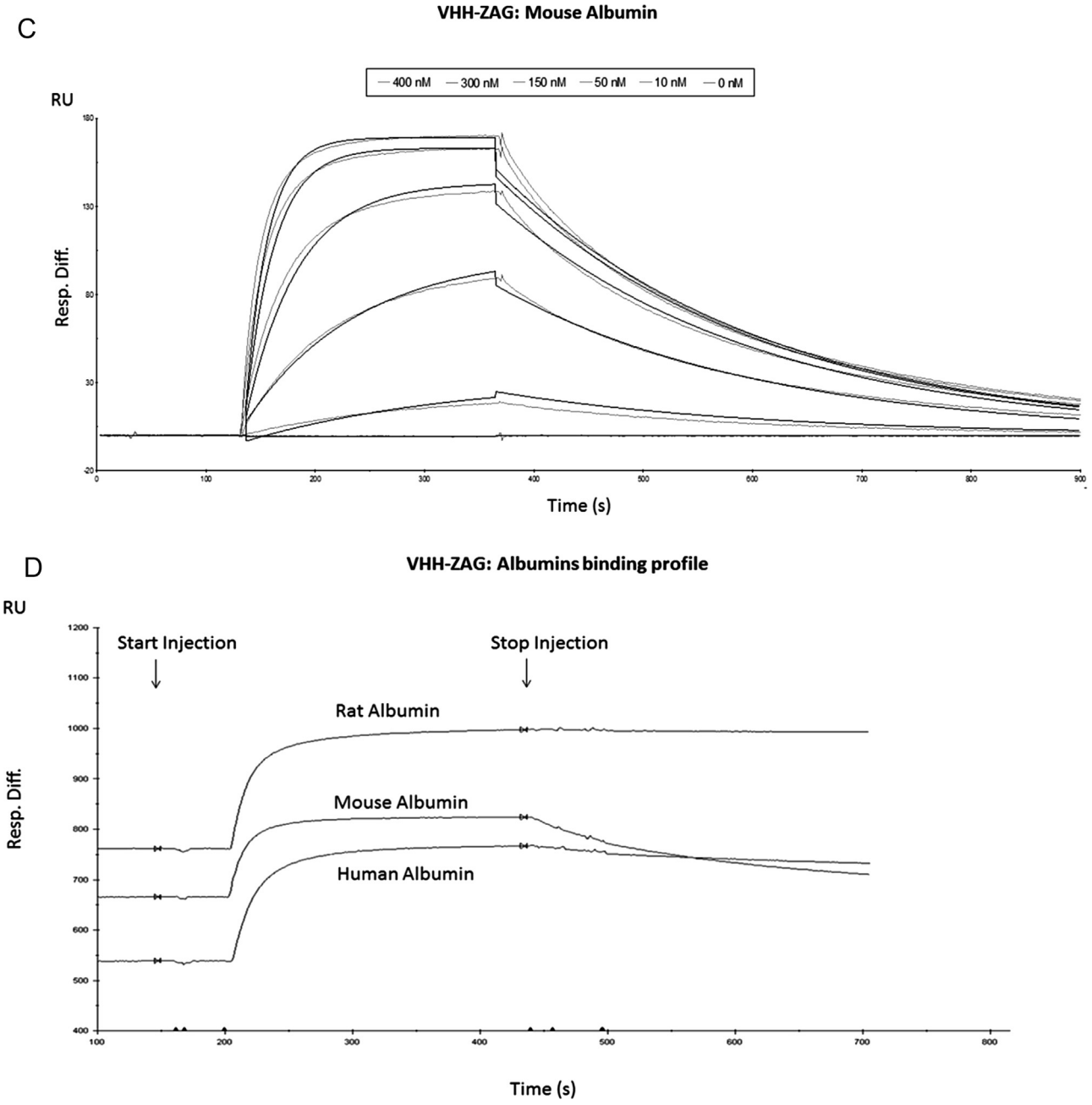

Fig. 4. (*continued*)

and 40.6 nM, respectively. These affinities values were similar to those obtained in previous studies, for the streptococcal protein G ABD (Johansson et al., 2002; Linhult et al., 2002; Stork et al., 2007). The SEC results indicated also the formation of VHH-Zag/albumin complexes *in vitro* with an increased hydrodynamic radius, confirming the albumin binding of VHH-Zag. These findings support the proposal that VHH-Zag uses the albumin binding to achieve extension of the circulation time, probably triggered by the reduced renal clearance and FcRn-mediated recycling mechanism. Accordingly, a previous study using the ABD from protein G in fusion with a single-chain

Table 1
Binding parameters of VHH-Zag against HSA, RSA and MSA. Association (kon) and dissociation (koff) rate constants were determined using surface plasmon resonance. The dissociation constant (Kd) was calculated from koff/kon.

Protein	*Kon* ($M^{-1}s^{-1}$)	*Koff* (s^{-1})	*Koff*/Kon	K_D (nM)
HSA	$8.68 \times 10^4 \pm 0.42$	$3.96 \times 10^{-4} \pm 0.07$	$4.57 \times 10^{-9} \pm 0.22$	4.57 ± 0.22
RSA	$1.06 \times 10^5 \pm 0.02$	$4.41 \times 10^{-5} \pm 0.08$	$4.15 \times 10^{-10} \pm 0.01$	0.42 ± 0.01
MSA	$9.88 \times 10^4 \pm 0.18$	$4.26 \times 10^{-3} \pm 0.14$	$4.06 \times 10^{-8} \pm 0.12$	40.6 ± 0.12

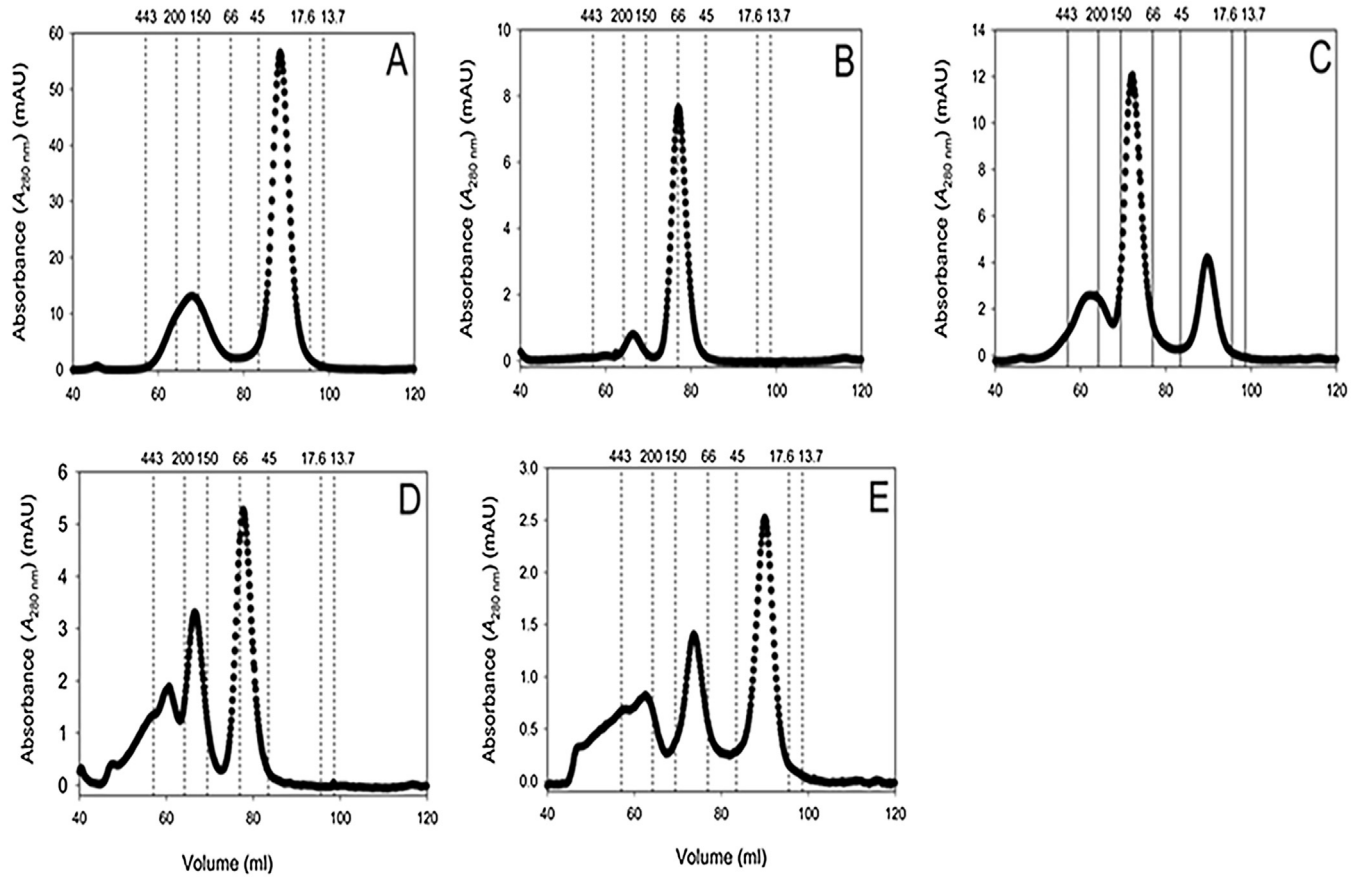

Fig. 5. Formation of VHH-Zag/albumin complexes. Size exclusion chromatography analysis of VHH-Zag (A), HSA (B), VHH-Zag/HSA complex (C), MSA (D) and VHH-Zag/MSA complex (E). VHH-Zag was incubated at equimolar concentrations with HSA or MSA in PBS at room temperature. Peak positions of marker proteins are indicated.

diabody for circulation time extension confirmed that the long half-life of this therapeutic protein may occur through the albumin-mediated FcRn recycling (Stork et al., 2009). Although VHH-Zag maintains the albumin binding capacities of the original ABD (Jonsson et al., 1995), the TNFα neutralization assays showed that the Zag fusion did not affect the efficacy of the anti-TNFα VHH. Our results indicate that the TNFα and albumin-binding abilities of the parental anti-TNFα VHH single-domain were retained in the recombinant VHH-Zag fusion molecule. Furthermore, the fusion of Zag ABD molecule with VHH did not disturb the high thermal stability of the VHH. Serum stability studies also demonstrate the high stability in human and mouse serum of VHH and VHH-Zag proteins. Regarding the pharmacokinetics, when compared to VHH, VHH-Zag showed a surprising 39-fold increase of the terminal elimination half-life (47 min for VHH *vs.* 31 h for VHH-Zag). This half-life extension was confirmed when the VHH-Zag fusion protein could be detected in mouse serum until 72 h after injection, comparing with the limited presence of 2 h for VHH. Moreover, the organ distribution of $^{99m}Tc(CO)_3$-VHH and $^{99m}Tc(CO)_3$-VHH-Zag (Fig. 10) exhibit clearly a different biodistribution profile. We observed that $^{99m}Tc(CO)_3$-VHH rapidly clear from the blood and showed a high kidney accumulation after 5 min (Fig. 10A and Table 2 supplementary data). $^{99m}Tc(CO)_3$-VHH-Zag had a substantial increase blood residence, which also leads to increase values in all the other organs (Fig. 10 B and Table 3 supplementary data). These biodistribution results are consistent with a recent study that we publish using ^{67}Ga as radionuclide (Morais et al., 2014). In this study, we showed that the Zag ABD affects the pharmacokinetic properties of VHH with significant differences in blood clearance and total excretion. The biodistribution profile of ^{67}Ga-NOTA-VHH exhibited a rapid clearance from blood and most tissues. On the other hand, ^{67}Ga-NOTA-VHH-Zag presented a slow washout from blood, muscle and bone, and an accumulation in highly irrigated organs such as liver, spleen and lung (Morais et al., 2014).

Altogether our data clearly demonstrate that the Zag ABD half-life extension strategy can improve the pharmacokinetic properties of a short half-life molecule. Indeed, our data shows that the half-life of our VHH-Zag fusion molecule is slightly higher than the circulation times determined for a bispecific single-chain diabody fused with the ABD from streptococcal protein G (scDbCEACD3-ABD, half-life = 27.6 h) or fused with HSA (scDbCEACD3-HSA, half-life = 25.0 h) (Hopp et al., 2010; Stork et al., 2007). Nevertheless, it is important to mention that concerns with the immunogenicity of Zag albumin domain for therapeutic applications may occur since is from bacteria. For instance, the immunogenicity of the ABD of protein G, (amino acid sequence 254–299) was detected in mice strains (Sjölander et al., 1997). For

Table 2
Thermal stability of VHH and VHH-Zag.

Protein	Tm B – Mean (°C)	Tm B – Median (°C)	Tm D – Mean (°C)	Tm D – Median (°C)
VHH	71.53 ± 0.14	71.56 ± 0.14	72.34 ± 0.25	72.43 ± 0.25
VHH-Zag	69.77 ± 0.14	69.87 ± 0.14	70.24 ± 0.23	70.24 ± 0.23

Tm B – Calculated Boltzamnn melting temperature; Tm D – Calculated derivated melting temperature.

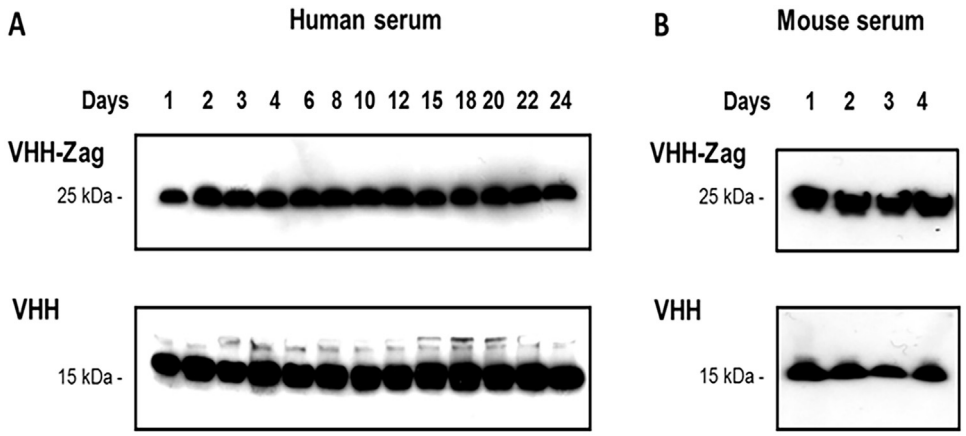

Fig. 6. *In vitro* stability in human and mouse serum of VHH and VHH-Zag. *In vitro* stability of the recombinant proteins was determined in human serum (A) and mouse serum (B) at 37 °C, during 24 days and 4 days, respectively. Proteins were detected by Western Blot, using an HRP-conjugated anti-HA mAb.

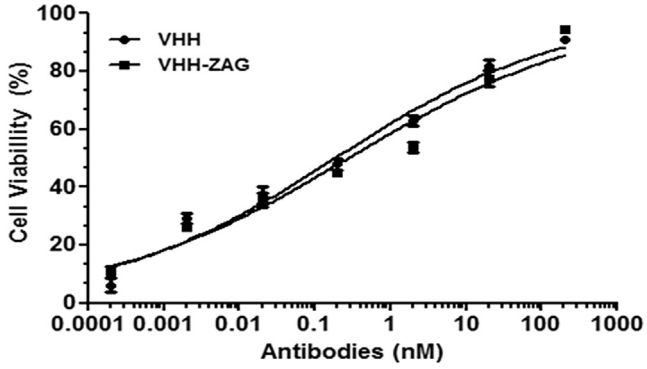

Fig. 7. Comparison of the ability of the VHH and VHH-Zag constructs to neutralize the cytolytic activity of TNFα. L929 cells were incubated with 1 ng/ml of TNF plus 1 μg/ml of actinomycin D in the presence of various concentrations of VHH or VHH-ZAG. After 24 h, the cell viability was determined using WST-1 reagent. Error bars correspond to standard deviation (n = 3).

therapeutic purposes, particularly in chronic diseases that required repeated injections, it will be necessary to reduce or ideally eliminate the immunogenicity. Several de-immunization strategies can minimize the immunogenicity of these ABDs (Baker and Jones, 2007). Ongoing de-immunization studies for the Zag ABD using Lonza's Epibase® *In*

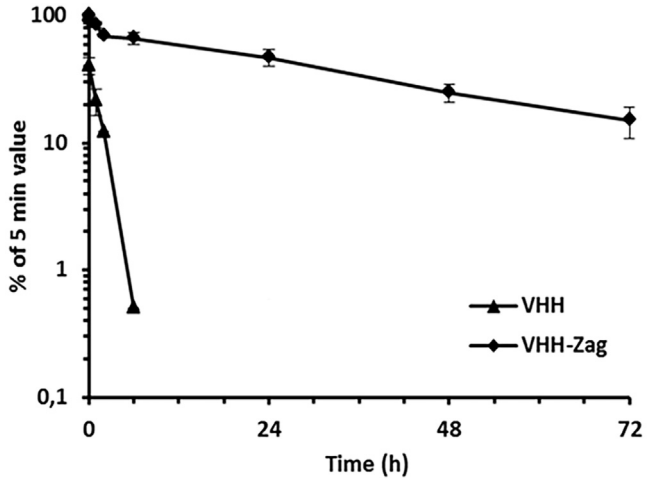

Fig. 8. Pharmacokinetic properties of VHH and VHH-Zag. VHH and VHH-Zag fusion proteins were injected separately into CD-1 mice (25 μg/animal) and serum analyzed at eight timepoints with n = 3 at each timepoint. The pharmacokinetic profiles of the antibodies constructs were calculated by ELISA. Data were normalized considering maximal concentration at the first time point (5 min).

Table 3
Pharmacokinetic parameters of VHH and VHH-Zag.

Protein	$t_{1/2}\alpha$ (h)	$t_{1/2}\beta$ (h)	$AUC_{(0\text{-}24h)}$ (%*h)
VHH	0.52 ± 0.25	0.79 ± 0.12	72.75 ± 7.35
VHH-Zag	3.21 ± 0.30	30.55 ± 0.14	1461.15 ± 152,98

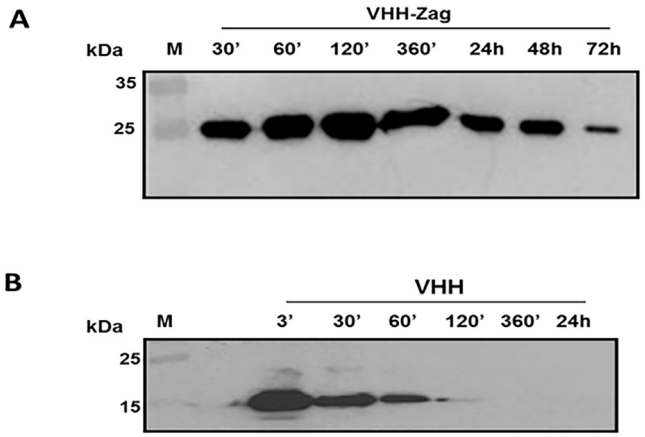

Fig. 9. *In vivo* detection of VHH and VHH-ZAG in mouse. *In vivo* detection of VHH-Zag (A) and VHH (B) was evaluated by Western Blot with anti-HA-tag antibody, in the mice serum samples collected during the pharmacokinetic assay at the different timepoints.

Silico platform may allow the identification of potential immunogenic epitopes in biotherapeutic proteins. Although the preliminary data reveals that there is a slight decrease in Zag affinity, albumin binding specificity and half-life extension properties of de-immunized Zag ABD seems to be similar to the wild-type Zag ABD (data not shown).

In conclusion, the present study demonstrates that the Zag ABD fusion is a promising strategy for half-life extension of rapidly cleared therapeutic recombinant antibody fragments. Moreover, we envision that this strategy can be potentially used as a universal method to improve the pharmokinetics properties of many others therapeutics proteins and peptides in order to improve their dosing schedule and clinical effects.

Acknowledgments

This work was financially supported by: Fundação para a Ciência e a

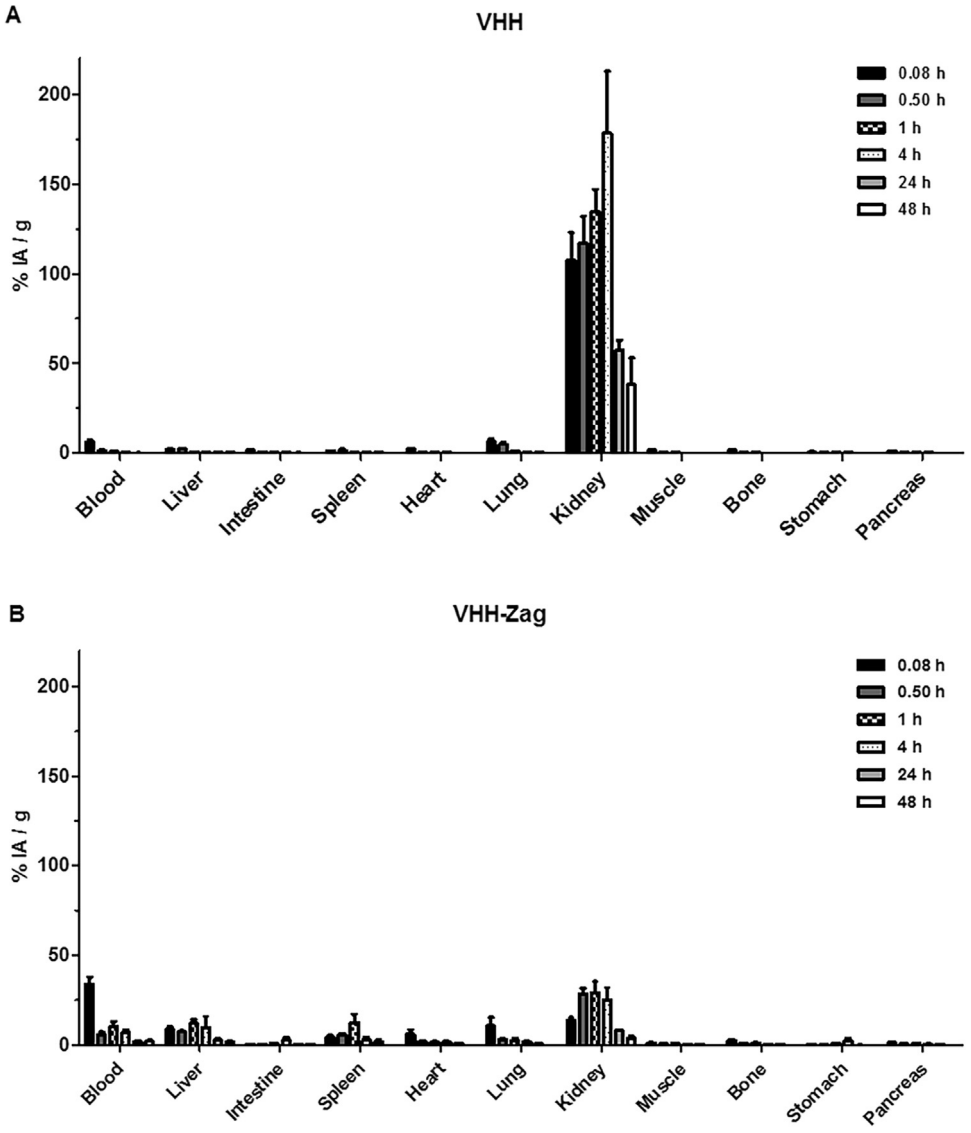

Fig. 10. Biodistribution $^{99m}Tc(CO)_3$-VHH and $^{99m}Tc(CO)_3$-VHH-Zag. Organ distribution of ^{99m}Tc-VHH (A) and ^{99m}Tc-VHH-Zag (B) proteins in CD-1 mice (n = 3).

Tecnologia (FCT), Portugal, (PTDC/SAU-FAR/115846/2009, IF/01010/2013/CP1183/CT0001 to F.A.S and IF/00268/2013/CP1173/CT0006 to M.S.), TechnoPhage S.A and Project LISBOA-01-0145-FEDER-007660("Microbiologia Molecular, Estrutural e Celular") funded by FEDER funds through COMPETE2020–"Programa Operacional Competitividade e Internacionalização" (POCI). C. Cantante e M. Morais thank the FCT for PhD fellowships (SFRH/BD/48598/2008 and SFRH/BD/48066/2008, respectively). We thank Dr. C. Xavier and Prof. V. Cavaliers for a generous gift of p-SCN-Bn-NOTA and fruitful discussions.

Appendix A. Supplementary data

Supplementary data associated with this article can be found, in the online version, at http://dx.doi.org/10.1016/j.jbiotec.2017.05.017.

References

Aires da Silva, F., Corte-Real, S., Goncalves, J., 2008. Recombinant antibodies as therapeutic agents: pathways for modeling new biodrugs. BioDrugs 22, 301–314.
Baker, M.P., Jones, T.D., 2007. Identification and removal of immunogenicity in therapeutic proteins. Curr. Opin. Drug Discov. Devel. 10, 219–227.
Barbas III, C.F., Burton, D.R., Scott, J.K., Silverman, G.J., 2001. Phage display: a laboratory manual. Cold Spring Harbor Laboratory Press.
Chen, C., Constantinou, A., Deonarain, M., 2011. Modulating antibody pharmacokinetics using hydrophilic polymers. Expert Opin. Drug Deliv. 8, 1221–1236. http://dx.doi.org/10.1517/17425247.2011.602399.
Dennis, M.S., Zhang, M., Meng, Y.G., Kadkhodayan, M., Kirchhofer, D., Combs, D., Damico, L.A., 2002. Albumin binding as a general strategy for improving the pharmacokinetics of proteins. J. Biol. Chem. 277, 35035–35043. http://dx.doi.org/10.1074/jbc.M205854200.
Goel, N., Stephens, S., 2010. Certolizumab pegol. mAbs 2, 137–147.
Holt, L.J., Basran, A., Jones, K., Chorlton, J., Jespers, L.S., Brewis, N.D., Tomlinson, I.M., 2008. Anti-serum albumin domain antibodies for extending the half-lives of short lived drugs. Protein Eng. Des. Sel. PEDS 21, 283–288. http://dx.doi.org/10.1093/protein/gzm067.
Hopp, J., Hornig, N., Zettlitz, K.A., Schwarz, A., Fuss, N., Müller, D., Kontermann, R.E., 2010. The effects of affinity and valency of an albumin-binding domain (ABD) on the half-life of a single-chain diabody-ABD fusion protein. Protein Eng. Des. Sel. PEDS 23, 827–834. http://dx.doi.org/10.1093/protein/gzq058.
Johansson, M.U., Frick, I.-M., Nilsson, H., Kraulis, P.J., Hober, S., Jonasson, P., Linhult, M., Nygren, P.-A., Uhlén, M., Björck, L., Drakenberg, T., Forsén, S., Wikström, M., 2002. Structure, specificity, and mode of interaction for bacterial albumin-binding modules. J. Biol. Chem. 277, 8114–8120. http://dx.doi.org/10.1074/jbc.M109943200.
Jonsson, H., Lindmark, H., Guss, B., 1995. A protein G-related cell surface protein in Streptococcus zooepidemicus. Infect. Immun. 63, 2968–2975.
Kontermann, R.E., 2009. Strategies to extend plasma half-lives of recombinant antibodies: bioDrugs Clin. Immunother. Biopharm. Gene Ther. 23, 93–109.
Kontermann, R.E., 2011. Strategies for extended serum half-life of protein therapeutics. Curr. Opin. Biotechnol. 22, 868–876. http://dx.doi.org/10.1016/j.copbio.2011.06.012.
Kontermann, R.E., 2016. Half-life extended biotherapeutics. Expert Opin. Biol. Ther. 16, 903–915. http://dx.doi.org/10.1517/14712598.2016.1165661.

Linhult, M., Binz, H.K., Uhlén, M., Hober, S., 2002. Mutational analysis of the interaction between albumin-binding domain from streptococcal protein G and human serum albumin. Protein Sci. Publ. Protein Soc. 11, 206–213. http://dx.doi.org/10.1110/ps.02802.

Morais, M., Cantante, C., Gano, L., Santos, I., Lourenço, S., Santos, C., Fontes, C., Aires da Silva, F., Gonçalves, J., Correia, J.D.G., 2014. Biodistribution of a (67)Ga-labeled anti-TNF VHH single-domain antibody containing a bacterial albumin-binding domain (Zag). Nucl. Med. Biol. 41, e44–e48. http://dx.doi.org/10.1016/j.nucmedbio.2014.01.009.

Nygren, P.A., Ljungquist, C., Trømborg, H., Nustad, K., Uhlén, M., 1990. Species-dependent binding of serum albumins to the streptococcal receptor protein G. Eur. J. Biochem. FEBS 193, 143–148.

Schlereth, B., Fichtner, I., Lorenczewski, G., Kleindienst, P., Brischwein, K., da Silva, A., Kufer, P., Lutterbuese, R., Junghahn, I., Kasimir-Bauer, S., Wimberger, P., Kimmig, R., Baeuerle, P.A., 2005. Eradication of tumors from a human colon cancer cell line and from ovarian cancer metastases in immunodeficient mice by a single-chain Ep-CAM-/CD3-bispecific antibody construct. Cancer Res. 65, 2882–2889. http://dx.doi.org/10.1158/0008-5472.CAN-04-2637.

Silence, K., Lauwereys, M., de Hans, H., 2004. Single-domain antibodies directed against tumor necrosis factor-alpha and uses therefore, United States Patent Application Publication, US 2.

Sjöbring, U., 1992. Isolation and molecular characterization of a novel albumin-binding protein from group G streptococci. Infect. Immun. 60, 3601–3608.

Sjölander, A., Nygren, P.A., Stahl, S., Berzins, K., Uhlen, M., Perlmann, P., Andersson, R., 1997. The serum albumin-binding region of streptococcal protein G: a bacterial fusion partner with carrier-related properties. J. Immunol. Methods 201, 115–123.

Stork, R., Müller, D., Kontermann, R.E., 2007. A novel tri-functional antibody fusion protein with improved pharmacokinetic properties generated by fusing a bispecific single-chain diabody with an albumin-binding domain from streptococcal protein G. Protein Eng. Des. Sel. PEDS 20, 569–576. http://dx.doi.org/10.1093/protein/gzm061.

Stork, R., Campigna, E., Robert, B., Müller, D., Kontermann, R.E., 2009. Biodistribution of a bispecific single-chain diabody and its half-life extended derivatives. J. Biol. Chem. 284, 25612–25619. http://dx.doi.org/10.1074/jbc.M109.027078.

Strohl, W.R., 2015. Fusion proteins for half-Life extension of biologics as a strategy to make biobetters. BioDrugs Clin. Immunother. Biopharm. Gene Ther. 29, 215–239. http://dx.doi.org/10.1007/s40259-015-0133-6.